



# Enhanced asphaltene degradation using piezocatalytic technology: A novel approach for sustainable oilfield operations

Wrea Muhammed Ibrahim<sup>a</sup>, Omid Amiri<sup>b,\*</sup>, Sangar S. Ahmed<sup>a</sup>, Hunar Yasin Muhammed<sup>a</sup>, Peshawa H. Mahmood<sup>c</sup>, Karzan A. Qurbani<sup>d</sup>, Nabaz A. Abdulrahman<sup>e</sup>, Karim A. Younis<sup>a</sup>, Peshang Kh Omer<sup>c</sup>

<sup>a</sup> Chemistry Department, College of Science, Salahaddin University, Kirkuk Road, 44001, Erbil, Kurdistan Region, Iraq

<sup>b</sup> Department of Medical Biochemical Analysis, Cihan University-Erbil, Kurdistan Region, Iraq

<sup>c</sup> Chemistry Department, College of Science, University of Raparin, Rania, Kurdistan Region, Iraq

<sup>d</sup> Department of Biology, College of Sciences, University of Raparin, Kurdistan of Iraq, Iraq

<sup>e</sup> Department of Petroleum and Mining Engineering, Faculty of Engineering, Tishk International University, Erbil, Iraq

## ARTICLE INFO

### Keywords:

Piezo catalyst  
Degradation  
Asphaltene  
Kinetic  
Mechanism

## ABSTRACT

Asphalt or oil spills containing asphaltene can contaminate soil, water bodies, and ecosystems. Natural balances are disrupted by this contamination. Asphaltene contaminates water sources such as rivers, lakes, and aquifers, making them unfit for human consumption. Aquatic habitats are damaged, and aquatic organisms cannot reproduce, grow, or maintain health. Air pollutants, including sulfur dioxide, nitrogen oxides, volatile organic compounds, and particulate matter, are released when asphaltene-containing materials are burned. Here, we have developed a new method for the degradation of asphaltene that is fast, clean, and cost-effective. The asphaltene was degraded using Ni<sub>x</sub>Mn<sub>y</sub>O piezo catalyst in this study. By using Ni<sub>x</sub>Mn<sub>y</sub>O under mechanical force, the result showed that asphaltene was degraded to the extent of 94.7 %. Piezo based on Ni<sub>x</sub>Mn<sub>y</sub>O has shown promising reusability when compared to conventional catalysts. Despite being used for 11 runs, it maintained 94% of its activity for 11 consecutive cycles. As well as analyzing the kinetics and thermodynamics of piezo asphaltene degradation, a mechanism pathway was developed for piezo degradation of asphaltene. Radical scavenger experiments showed that superoxide radicals, holes, and hydroxyl radicals are involved in the degradation of asphaltene by Ni<sub>x</sub>Mn<sub>y</sub>O piezo catalysts. However, hydroxyl radicals and holes are responsible for the majority of asphaltene degradation.

## 1. Introduction

In the course of oil production, asphaltene can precipitate and deposit. This may result in various problems, including pore plugging, reduced productivity, pipeline obstruction, and malfunctions of surface equipment [1–3]. Thus, it is essential that asphaltene be removed from the oil production process in order to maintain efficiency and safety. To address asphaltene deposition, two main approaches can be taken: removal and prevention [4–6]. There are several methods available for removing deposits, including mechanical, thermal, chemical, and ultrasonic methods that are designed to dissolve or dislodge the deposits from the affected areas. A chemical inhibitor or dispersant can prevent or delay the precipitation or aggregation of asphaltene molecules in the oil phase by preventing or delaying the precipitation of asphaltene

molecules [7–10]. Also, asphaltene inhibition helps to control Asphaltene deposits that eventually stop oil flow [11,12].

There are, however, some limitations and challenges associated with both removal and prevention methods, including high costs, environmental impact, damage to the formation, compatibility issues, and varying efficiency levels [13–17]. As a result, researchers are investigating new methods of improving the performance of these methods and reducing their shortcomings, such as using nanomaterials that are capable of enhancing the solubility, stability, and dispersibility of asphaltene in oil.

Hydrocarbons, such as asphaltene, are also among the substances that contribute to water and soil pollution [18–20]. Due to this, it is necessary to remediate spills that are related to petroleum to minimize their harmful effects on the environment. Various methods of

\* Corresponding author.

E-mail addresses: [o.amiri1@gmail.com](mailto:o.amiri1@gmail.com), [oamiri@uor.edu.krd](mailto:oamiri@uor.edu.krd) (O. Amiri).

<https://doi.org/10.1016/j.rineng.2024.101938>

Received 17 January 2024; Received in revised form 14 February 2024; Accepted 20 February 2024

Available online 21 February 2024

2590-1230/© 2024 The Authors. Published by Elsevier B.V. This is an open access article under the CC BY-NC license (<http://creativecommons.org/licenses/by-nc/4.0/>).

remediation are available, including physical, chemical, biological, and combinations of these methods [21–23]. A physical method involves the use of adsorbent materials to contain the spill or to physically remove the oil, while a chemical method involves the use of chemicals for coagulation and solubilization. The chemical remediation of hydrocarbons is commonly carried out by the use of ionic/anionic surfactants, such as Span 80, Tween 80, Tween 85, and dioctyl sodium sulfosuccinate [24,25]. Hydrocarbon-contaminated sites are also treated with surfactants to improve the solubility and flow properties of oils, which can result in their physical removal or natural degradation. It is, however, extremely labor intensive and therefore considered inefficient to physically remove hydrocarbons from contaminated sites. There are also disadvantages associated with chemical methods, such as the need for expensive and toxic chemicals that can accumulate and remain in the environment for a long period of time [26,27]. A new method was developed here that did not require expensive materials in order to degrade and remove asphaltene. Additionally, it is an environmentally friendly and clean method. Here,  $Ni_xMn_yO$  Piezo-catalysts were used to degrade asphaltene, which is a green process.

The piezocatalysts are a type of catalyst capable of being activated or enhanced by mechanical forces, such as pressure or vibration [28–31]. Piezo refers to the piezoelectric effect, which occurs when certain materials generate an electric charge when mechanical stress is applied.

The piezoelectric effect is used by piezo catalysts to enhance their catalytic activity [32,33]. The application of mechanical force to the catalyst causes changes in its crystal structure or electronic properties, resulting in improved catalytic performance. Compression,  $ZrO_2$  balls, ultrasonic vibration, or mechanical agitation can all be used to apply this mechanical force [34–37].

There are several advantages to using piezo catalysts compare to the photocatalysts [38–40]. As a first benefit, it facilitates the activation of catalytic reactions without the use of high temperatures or harsh chemical conditions. As a result, energy consumption can be reduced and reaction conditions can be milder. Second, piezo catalysts can exhibit higher catalytic activity and selectivity than traditional catalysts, thereby improving the efficiency of reactions. Furthermore, it is a clean and environmentally friendly process. Last but not least, piezo catalysts can be easily incorporated into systems in which mechanical force is readily available, such as flow systems or mechanical devices [41–45].

In this study, we prepared  $Ni_xMn_yO$  piezo catalysts by a simple microwave method and applied them to the degradation of asphaltene. It has been demonstrated that parameters such as the cycling time, the concentration of precursors, and microwave power have an impact on the morphology and chemical composition of  $Ni_xMn_yO$  piezo catalysts. By adjusting the morphology and chemical composition of the catalyst, it was found that a high asphaltene degradation yield of 94.7% could be achieved. In terms of kinetics, piezo asphaltene degradation is governed by a second-order kinetic law, and the reaction has nearly completed after the first 40 min.

## 2. Experimental

### 2.1. Materials

There was no further purification of the chemicals used in this study because all of them were analytical grade. nickel precursor (Nickel(II) Chloride Hexahydrate) was obtained from BDH Chemicals (England), as was a hexahydrate of Potassium Permanganate ( $KMnO_4$ ), and a disodium salt of ethylenediaminetetraacetic acid (EDTA-2Na). 1, 4-benzoquinone (BQ), and isopropanol (IPA). Alpha (India) provided an  $NH_4OH$  ammonium hydroxide solution.

### 2.2. Synthesis of $Ni_xMn_yO$ piezo catalysts

1 mmol of Ni precursor (as per Table 1) was dissolved in 30 mL of distilled water to create Solution A. In a separate beaker, 1 mmol Mn

**Table 1**

Experimental details for synthesis of  $Ni_xMn_yO$  by microwave method.

Sample	Microwave cycling time (on: off/sec)	Microwave power (W)	[Ni] and [Mn] (mmol)	Ammonia (mmol)	Solvent
N1	120: 30	700	1	4	Water
N2	120: 60				
N3	120: 120				
N4	120: 30	700	2	4	Water
N5			4		
N6	120: 30	700	1	6	Water
N7				8	
N8	120: 30	540	1	4	Water
N9		385			
N10	120: 30	700	1	4	Ethanol/ Water

precursor (as per Table 1) was dissolved in 30 mL of distilled water to create Solution B. Then, mixed Solutions A and B were mixed and stirred for 10 min. Next, the appropriate amount of aqueous ammonia solution was added (as per Table 1) and stirred for 5 min. Then, the mixture was microwaved for 30 min before washing and drying it. Lastly, products were calcinated at 450 °C for 3 h. We studied the effect of different parameters including cycling time, precursor concentration, microwave power, and time on the morphology and compound of final products.

### 2.3. Piezocatalytically degradation of asphaltene

An ultrasonic device was used in a Pyrex cell to degrade asphaltene (30 ppm) in 25 mL of model fuel (asphaltene)/toluene solution containing 100 mg of piezocatalyst. Prior to ultrasonication, the samples were stirred for 30 min in the dark. The purpose of this step is to establish an equilibrium between adsorption and desorption. After a certain period of time, degraded samples were withdrawn from the catalyst and centrifuged in a volume of 10 mL to determine their degradation state. ACL-2, Tanaka (Japan) colorimeter model was used to analyze the model asphaltene after degradation. Furthermore, radical trapping experiments were conducted during piezo degradation of asphaltene in order to identify the primary active species. Scavengers such as  $Na_2EDTA$ , IPA, and BQ were added to the fuel system in order to quench  $h^+$ , OH radicals, and oxygen radicals.

### 2.4. Characterization of $Ni_xMn_yO$ piezo catalysts

An X-ray diffractometer (Philips X'pert Pro MPD, The Netherlands) was used to analyze the crystal structure of the samples. The radiation used was Ni-filtered  $Cu K\alpha$  radiation ( $\lambda = 1.54 \text{ \AA}$ ). An ultrasonic bath of a 20 kHz ultrasonic device rated at 250 W was used to perform the sonochemical reaction. X-Max Oxford, England, was used to perform the EDS analysis (energy dispersion spectroscopy). FESEM images were recorded using the IGMA/VP system from ZEISS, Germany. A transmission electron microscope (TEM, Zeiss) was used to obtain TEM images.

## 3. Results and discussions

### 3.1. Characterization of $Ni_xMn_yO$ piezo-catalyst

As far as we know, this is the first report on the degradation of asphaltenes by a piezo catalyst. In order to accomplish this,  $Ni_xMn_yO$  Piezo catalysts were prepared by fast, simple, and energy-saving microwave techniques. In the first step of the investigation, we examined the effect of the following parameters on the morphology and chemical composition of final Piezo catalysts: 1. microwave cycling time effect, 2. the concentration of precursors, 3. the ammonia concentration effect, and 4. the power of the microwave. According to XRD results (Fig. 1), changing synthesis parameters may affect x and y in  $Ni_xMn_yO$  structures;

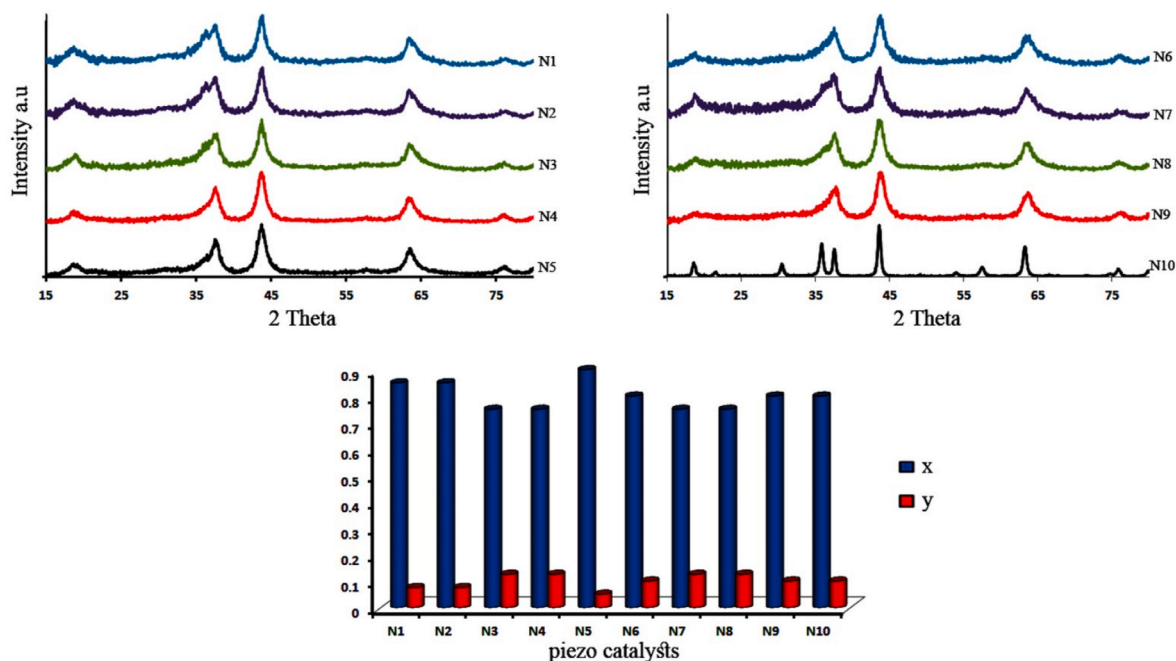


Fig. 1. XRD patterns of prepared catalysts a) N1– N5, b) N6–N10, and c) x and y value for N1–N10.

however, the phase of catalysts does not change. The crystal size of  $\text{Ni}_x\text{Mn}_y\text{O}$  piezocatalysts was also affected by synthesis parameters. Detailed information about the chemical composition, phase, and crystal size of all catalysts was presented in Table 2. X and y in  $\text{Ni}_x\text{Mn}_y\text{O}$  piezocatalysts was calculated based on XRD data. As part of the synthesis of  $\text{Ni}_x\text{Mn}_y\text{O}$  piezocatalysts, three different cycling times were examined on the chemical composition and crystal size of the piezo catalyst, including 2 min on followed by 30 s off, 2 min on followed by 1 min off, and 2 min on followed by 2 min off. Increasing the off time between each cycle resulted in a decrease in x and an increase in y values. Furthermore, by increasing the off time, crystal sizes were reduced. In addition, Fig. S1 indicates that the catalysts were almost amorphous prior to being calcined at 450 °C for 3 h.

Increasing the concentration of Ni and Mn precursors first resulted in a decrease in the x value and an increase in the y value, and then an

Table 2

Detailed information about the chemical composition, phase, and crystal size of all catalysts.

Sample	Chemical Formula	Phase	JCPDS	Group Space	Crystal Size (nm)
N1	$\text{Ni}_{0.85}\text{Mn}_{0.075}\text{O}$	Cubic	96-901-3978	F m -3 m	5.3
N2	$\text{Ni}_{0.85}\text{Mn}_{0.075}\text{O}$	Cubic	96-901-3978	F m -3 m	4.6
N3	$\text{Ni}_{0.75}\text{Mn}_{0.125}\text{O}$	Cubic	96-901-3976	F m -3 m	4.6
N4	$\text{Ni}_{0.75}\text{Mn}_{0.125}\text{O}$	Cubic	96-901-3976	F m -3 m	5.1
N5	$\text{Ni}_{0.9}\text{Mn}_{0.05}\text{O}$	Cubic	96-901-3979	F m -3 m	4.7
N6	$\text{Ni}_{0.8}\text{Mn}_{0.1}\text{O}$	Cubic	96-901-3977	F m -3 m	3.7
N7	$\text{Ni}_{0.75}\text{Mn}_{0.125}\text{O}$	Cubic	96-901-3976	F m -3 m	3.9
N8	$\text{Ni}_{0.75}\text{Mn}_{0.125}\text{O}$	Cubic	96-901-3976	F m -3 m	3.8
N9	$\text{Ni}_{0.8}\text{Mn}_{0.1}\text{O}$	Cubic	96-901-3977	F m -3 m	4.2
N10	$\text{Ni}_{0.8}\text{Mn}_{0.1}\text{O}$	Cubic	96-901-3977	F m -3 m	17.8

increase in the x value and a decrease in the y value. In addition, increasing the ammonia amount by 50% and 100% resulted in a decrease in the x value from 0.85 to 0.75 and an increase in the y value from 0.075 to 0.125. As far as crystal size is concerned, increasing the ammonia value first decreased and then increased the size of the crystal. When the volume of ammonia was increased by 50% and 100%, however, the size remained almost constant.

In the case of a decrease in microwave power from 700 W to 540 W, the x and y values were changed from 0.85 to 0.075 to 0.75 and 0.125, while the crystal size decreased from 5.3 nm to 3.8 nm. It was achieved by applying microwave power of 385 W that the x and y values of the crystal were 0.8 and 0.1, respectively, while the crystal size was 4.2 nm. Use mixing solvent also changed the values of x and y from 0.85 to 0.8 and 0.075 to 0.1, respectively.

An SEM analysis of N1–N10 was conducted to examine the effect of microwave cycling time, precursor ratio, ammonia concentration, and microwave power on piezo catalyst morphology. Fig. 2 a-i and Fig. 3 a-c present the results.

In SEM images, it was found that increasing the off time in each cycle did not significantly affect the morphology of the products. Almost spherical nanoparticles are the characteristic morphology of N1–N3 piezo catalysts. Increasing the off time in each microwave cycle, however, led to an increase in the size of prepared  $\text{Ni}_x\text{Mn}_y\text{O}$  nanostructures. XRD and SEM results indicated that changing the concentration of precursors has a significant impact not only on the chemical composition of products but also on their morphology. Upon doubled concentrations of nickel and manganese precursors, nanoparticles begin to assemble and form larger particles. Nanoparticles formed Nano-flower-like  $\text{Ni}_x\text{Mn}_y\text{O}$  nanostructures when nickel and manganese precursor concentrations were increased four-fold. The results of an investigation into the effect of ammonia concentration indicate that increasing ammonia concentration affects the chemical composition of the products rather than their morphology. We examined the effect of microwave power on the morphology of  $\text{Ni}_x\text{Mn}_y\text{O}$  nanostructures at three different microwave powers, including 700 W (N1), 540 W (N8), and 385 W (N9). According to Fig. 3 a and b, higher microwave power resulted in smaller nanoparticles, but it did not affect their morphology, and for all three microwave powers, spherical nanoparticles were obtained. Last but not least, the effect of solvent on the morphology of  $\text{Ni}_x\text{Mn}_y\text{O}$  nanostructures

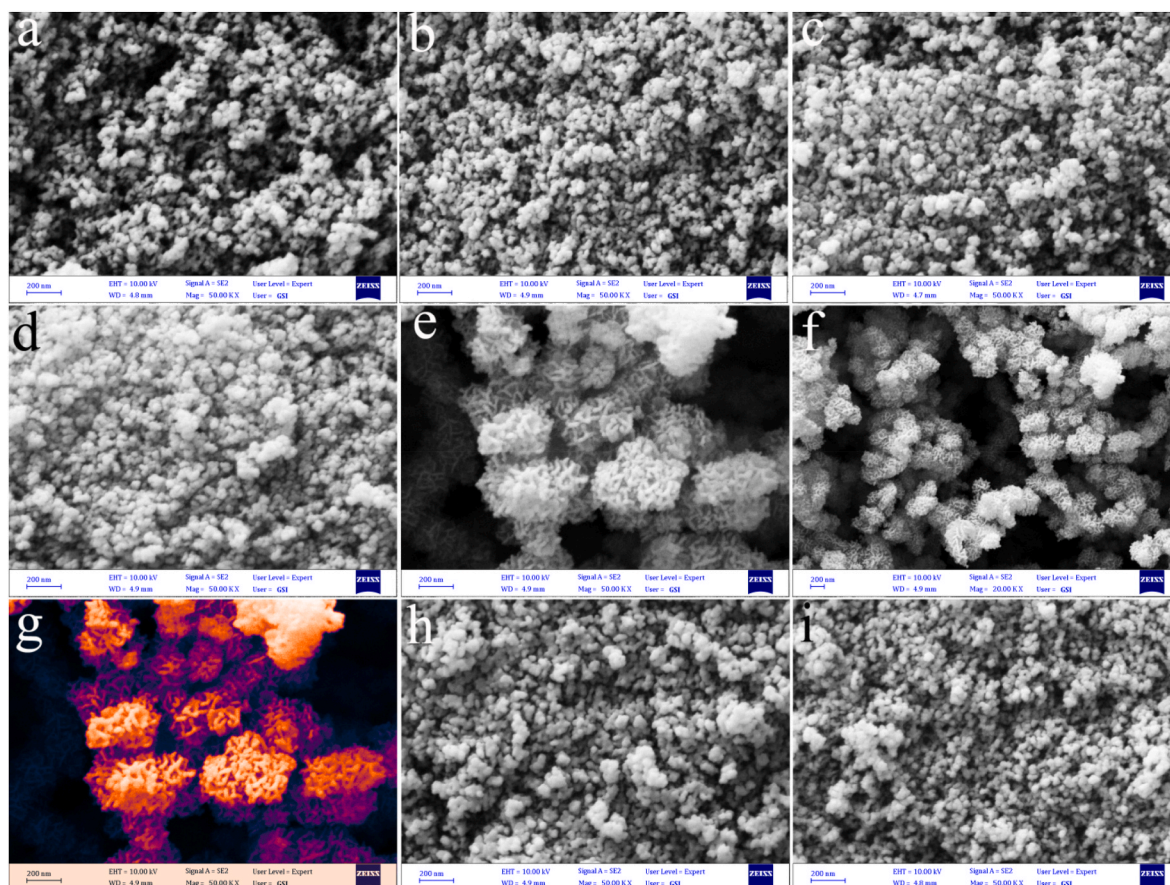


Fig. 2. SEM images for piezo catalysts N1–N10: a) N1, b) N2, c) N3, d) N4, e, f, g) N5, h) N6, and i) N7.

was investigated. To accomplish this, distilled water (N1) and a mixture of distilled water and ethanol (N10) were used to prepare  $Ni_xMn_yO$  nanostructures. It was found that particles were larger when mixed solvents were used (Fig. 3 c). It can be seen in Fig. 3 d that the champion  $Ni_xMn_yO$  piezo catalyst exhibited nanoparticles of 10–40 nm in diameter. Fig. 3 e-g illustrates the EDX results for N7, N3, and N5 which exhibited the highest piezo-catalytic activity regarding asphaltene degradation. In Fig. 3 h and i, the EDX results of N9 and N8 were shown, which showed the lowest level of piezo-catalytic activity regarding asphaltene degradation. A supporting document (Fig. S2) contains the EDX results of other samples.

### 3.2. Effect of synthesis parameters on the piezo degradation of asphaltene

In order to investigate the effect of cycling time, precursor concentration, microwave time, and solvent on asphaltene degradation efficiency (ADE), N1–N10 piezo catalysts were used to remove asphaltene from toluene. It should be notice that we examined the possibility of absorption of asphaltene over the catalyst by stirring the solution in the dark in the presence of prepared piezo catalysts. Results showed that up to 4% of asphaltene has been absorbed over a piezo catalyst that is nugatory. In addition, bare ultrasonic (without piezo catalysts) only degrades 1–2 % of asphaltene.

#### 3.2.1. Effect of off time in microwave cycle on degradation of asphaltene

To study the effect of off time in the microwave cycle on the degradation of asphaltene, N1, N2, and N3 samples were used for the degradation of asphaltene in toluene. The calibration curve of asphaltene in toluene was conducted prior to the degradation test of asphaltene by the prepared catalysts (Fig. S3). When the off time in each cycle was 30 s, asphaltene degradation efficiency was determined to be 87.1%. By

increasing the off time during catalyst synthesis to 1 min and 2 min, ADE was increased to 89.7% and 92.4 %, respectively (Fig. 4a). By comparing XRD, EDX, and SEM results of N1, N2, and N3, we can figure out that catalyst with bigger particle size and less Ni content showed higher ADE.  $Ni_xMn_yO$  appears to act as a dopant, and increasing the Mn content increases the asymmetry of the catalyst and increases its piezocatalytic activity.

#### 3.2.2. Effect of initial concentration of Ni and Mn on degradation of asphaltene

By doubling and quadrupling the initial concentration of Ni and Mn, we examined the effect of precursor concentration on the piezo catalytic activity of  $Ni_xMn_yO$  nanostructures. In this study, the results indicated that the piezo degradation rate of asphaltene was increased when Ni and Mn concentrations were increased (Fig. 4 b). By doubling the initial concentration of Ni and Mn, asphaltene degradation rate increased from 87.1% to 89.5 %. XRD and SEM results showed that doubling Ni and Mn concentration led to decrease the Ni amount in piezo catalyst and increase crystal size. More increasing the Ni and Mn concentrations led to change the morphology of products and flower like structures were formed. This could explain the higher asphaltene degradation rate despite increasing the Ni amount in N5. As a result of the intricate morphology of flower-like structures, several factors can affect their piezoelectric behavior, such as surface area, crystal orientation, Strain distribution, flexibility, polarization alignment. Due to their intricate morphology, flower-like structures often have a large surface area. Increasing the surface area of a material can enhance its interaction with external mechanical forces, resulting in improved piezoelectric performance. It is important to note that the piezoelectric properties of a material are strongly influenced by its crystal structure and orientation. The arrangement of petals or branches in flower-like structures may

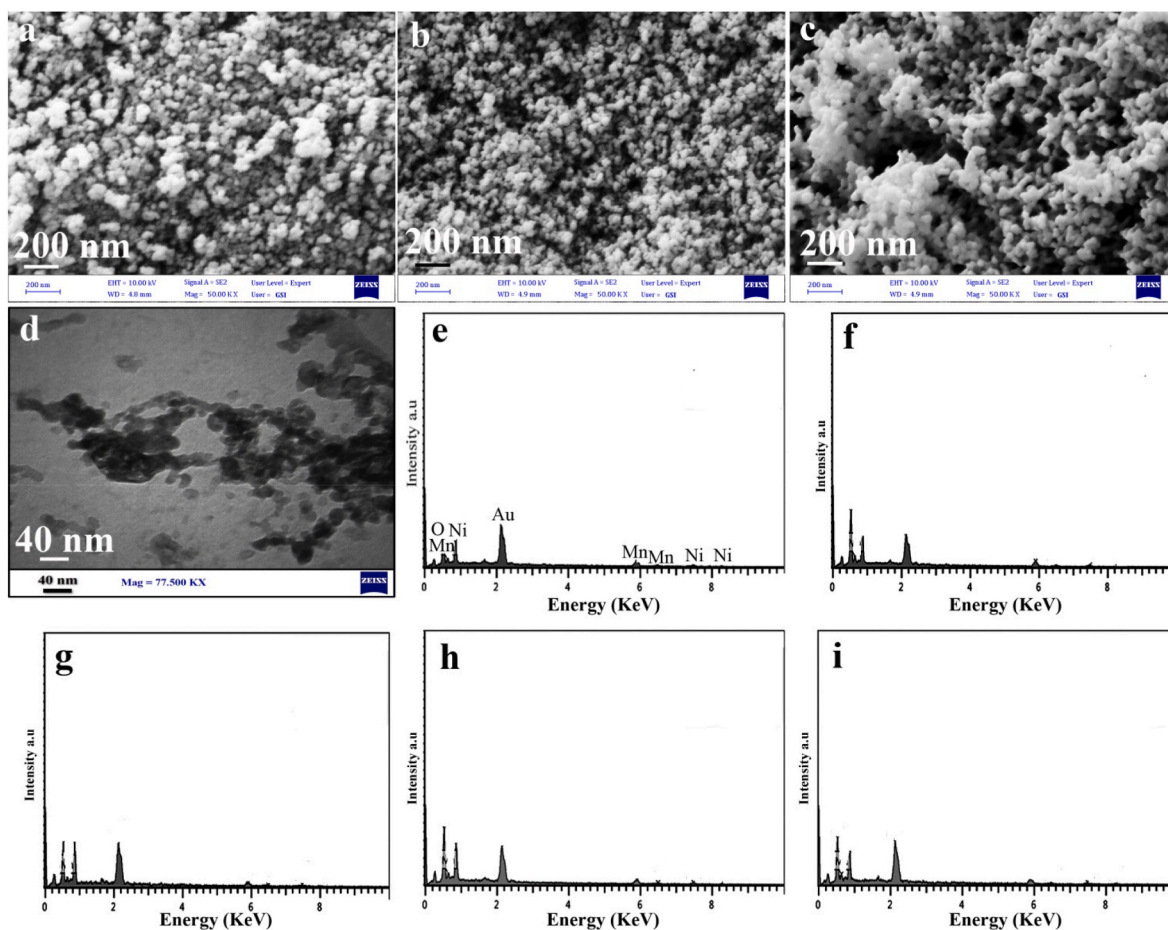


Fig. 3. SEM images of a) N8, b) N9, and c) N10. d) TEM images of N7 as a champion piezo catalyst. EDX results of e) N7, f) N3, g) N5 showed the highest catalytic activity, and h) N9, i) N10 showed the lowest catalytic activity.

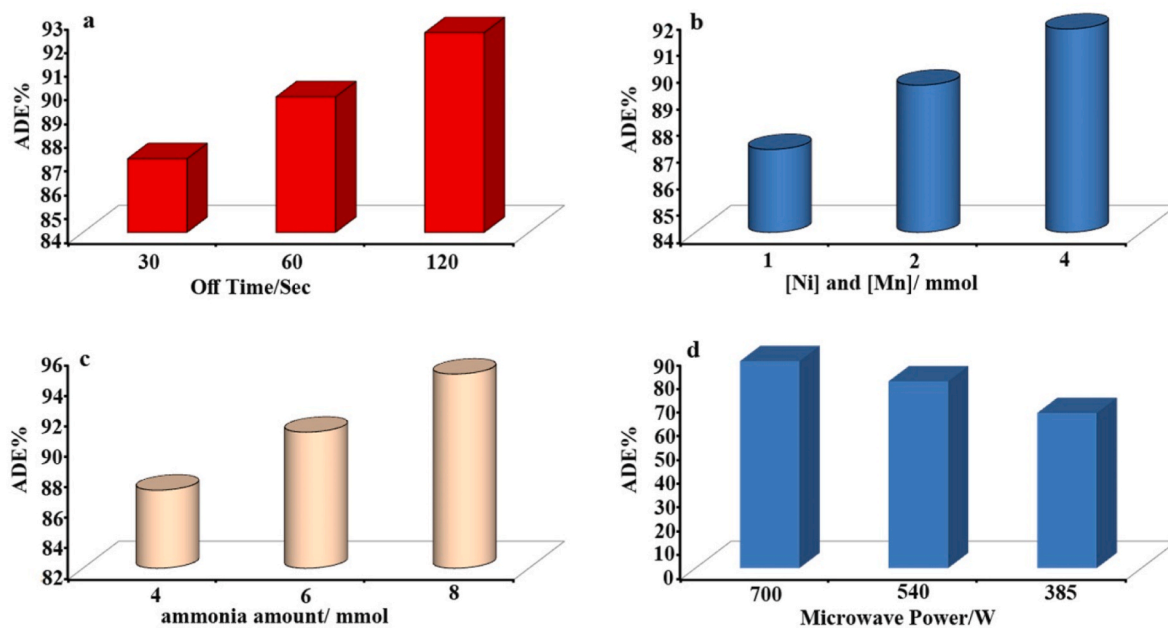


Fig. 4. Effect of synthesis parameters on degradation efficiency of asphaltene including a) off time in each microwave cycle, b) amount of Ni and Mn in precursors, c) amount of ammonia, and d) microwave power.

affect the crystallographic orientations, which may affect piezoelectric properties. Compared to single-crystal counterparts, piezoelectric properties can be enhanced by multiple orientations. There can be variations in strain distribution throughout the material due to the complex morphology of flower-like structures. As a result of the non-uniform strain distribution, localized electric fields may be generated, resulting in an enhanced piezoelectric effect. Because of their unique architecture, flower-like structures are often flexible. In response to mechanical stress, flexibility allows for a greater degree of deformation, resulting in increased piezoelectric response. An alignment of the polarization of the piezoelectric material is essential to ensure the material exhibits significant piezoelectric properties. A flower-like morphology can facilitate the alignment of polarized domains, resulting in improved piezoelectric performance.

### 3.2.3. Effect of initial concentration of ammonia on degradation of asphaltene

By applying three different concentrations of ammonia during the synthesis of  $Ni_xMn_yO$  nanostructures, we investigated the effect of ammonia concentration on the piezo degradation of asphaltene. In accordance with the results presented in Fig. 4 c, increasing ammonia concentration led to an improvement in asphaltene degradation. 87.1% of asphaltene degradation was observed when the amount of ammonia was 4 mmol. The degradation rate was boosted to 90.9 % by increasing the amount of ammonia by 50 percent. Increasing the ammonia amount by 100 percent was eventually able to achieve a 94.7 % efficiency rate. XRD results indicate that N7, which shows the highest degradation efficiency when it comes to asphaltene, has the lowest Ni content, while N1, which shows the highest Ni content, has the lowest asphaltene degradation efficiency.

### 3.2.4. Effect of microwave power on degradation of asphaltene

Microwave power was considered as another parameter that could affect the piezo catalytic activity of  $Ni_xMn_yO$  nanostructures. We studied the effect of microwave power by applying N1, N8, and N9 as piezo catalyst to degrade asphaltene. Related results are illustrated in Fig. 4 d.

Based on the results, asphaltene degradation was decreased by decreasing microwave power. Asphaltene degradation efficiency was 87.1%, 78.6, and 65.3 % when microwave power was 700 W, 540 W, and 385 W, respectively. Various studies have demonstrated that higher microwave power can result in greater crystallinity because more energy can be provided for crystal nucleation and growth [46–48]. Further, it has been demonstrated that higher microwave power enhances the optical and catalytic properties of nanomaterials, as it improves the rate of charge transfer and separation [46–48]. Thus, N1 may display better piezo activity due to its higher crystallinity and higher charge transfer.

### 3.3. Effect of operation conditions on the degradation efficiency of asphaltene

There are several parameters that could affect the asphaltene degradation rate during piezo catalytic teste including catalyst dosage, asphaltene concentration, ultrasonic power, and ultrasonic time. Utilizing N3 as the piezo catalyst and 300 W of ultrasonic power, we systematically examined the effect of these parameters on the degradation efficiency of 30 ppm asphaltene.

#### 3.3.1. Effect of $Ni_xMn_yO$ dosage on the degradation efficiency of asphaltene

There is a significant effect that can be made on the kinetics of a reaction and the overall efficiency of the process depending on the amount and dosage of catalyst used. In order to assess the effect of  $Ni_xMn_yO$  dosage on asphaltene degradation efficiency, four catalyst dosages of 0.4 g/L, 1 g/L, 2 g/L, and 4 g/L were used in piezo degradation of asphaltene while maintaining the following parameters: asphaltene concentration was 30 ppm, ultrasonic power, and duration were 300 W and 2 h, respectively. Increasing  $Ni_xMn_yO$  dosage increased ADE rates, as shown in Fig. 5 a. When no piezo catalyst was used, bare ultrasonic treatment only degrades around 1% of asphaltene. By using 0.4 g/L of  $Ni_xMn_yO$  for the piezo degradation batch, an ADE% of 43.7 % was obtained. As a result of the low dosage of 0.4 g/L, the reaction appears to proceed slowly. Due to the lack of catalysts present, the reaction may not be able to take place effectively. As a result of the piezo

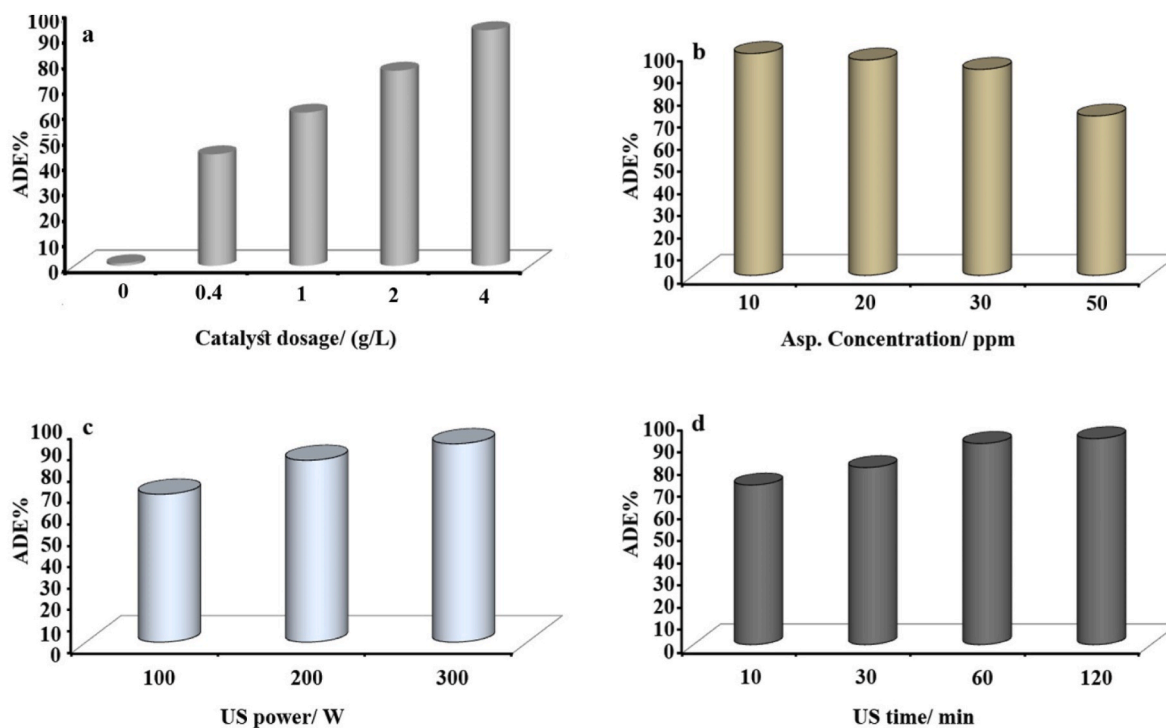


Fig. 5. Effect of operation parameters during piezo degradation of asphaltene on ADE%: a) catalyst dosage, b) asphaltene concentration, c) ultrasonic power, and d) ultrasonic irradiation time.

degradation test conducted with 1 g/L of  $\text{Ni}_x\text{Mn}_y\text{O}$ , ADE% increased by 37.5% and reached 60.1%. The ADE% increased further to 76.5 % and 92.4 % when the  $\text{Ni}_x\text{Mn}_y\text{O}$  dosage was increased to 2 g/L and 4 g/L. In general, the rate of the reaction increases with an increase in the catalyst dosage. The higher catalyst dosage allows a greater number of reactants to participate in a reaction by providing an alternative reaction pathway with lower activation energy. As a result, the reaction rate is accelerated.

### 3.3.2. Effect of asphaltene concentration on the piezo degradation efficiency

The degradation efficiency of catalysts can be affected significantly by the concentration of pollutants. The performance of catalysts is generally governed by the concentration of pollutants within a specific range. The effect of asphaltene concentrations on ADE% was studied using different asphaltene concentrations including 10, 20, 30, and 50 ppm (Fig. 5 b). ADE reaches 99.5% when a low amount of asphaltene (10 ppm) is present in toluene. As asphaltene content was increased to 20 ppm and 30 ppm, the ADE% decreased to 96.6% and 92.4%, respectively. As a final step, piezo degradation testing was conducted for asphaltene content of 50 ppm, which resulted in a decrease in ADE% to 71.5%. In this study, the ADE% was decreased by increasing asphaltene content since higher pollutant concentrations can saturate the active sites on the catalyst's surface [49,50], which results in a decrease in degradation efficiency. When the active sites are occupied by a high concentration of pollutants, the catalyst's ability to adsorb additional reactants and promote their degradation may be hindered. Due to overcrowding, high concentrations of pollutants can cause mass transport limitations, preventing the reactants from reaching the active sites efficiently [51,52]. The result may be a reduction in the amount of pollutants that are in contact with the catalyst surface, thereby limiting degradation efficiency.

### 3.3.3. Effect of ultrasonic power on the piezo degradation efficiency

It is well known that ultrasonic power has a significant impact on the catalytic activity of piezo catalysts. Ultrasonic waves generate mechanical vibrations which result in acoustic cavitation when applied to the catalyst [53,54]. In the catalyst solution, cavitation causes tiny bubbles to form and collapse. A microjet is created when bubbles collapse, generating localized high temperatures and pressures. By generating intense shear forces and turbulence within the solution, these microjets promote enhanced mass transfer and improve access to the catalyst's active sites for reactants. Cavitation and microjet formation are generally more vigorous at higher ultrasonic power levels. This increased mechanical energy can improve the catalytic activity by accelerating reaction rates and enhancing the efficiency of the catalytic process. Fig. 5 c illustrates the effects of ultrasonic power on the ADE%. According to the results, ADE% was 68.9 % when ultrasonic power was 100 W. When ultrasonic power was increased to 200 W, degradation efficiency improved to 84.7%. The degradation efficiency improved further to 92.4% when ultrasonic power was increased to 300 W. As ultrasonic power is increased, the diffusion and mass transfer of reactants to the catalytic sites is increased, resulting in an increase in ADE %. The catalytic activity can be enhanced by improving mass transfer. As well, an increase in ultrasonic power may result in fragmentation or dispersion of the piezo-catalyst particles, resulting in more surface area available for catalytic reactions. By reducing particle size or increasing dispersion, more active sites are available for reactant adsorption and reaction, thus improving the overall catalytic activity. A higher mechanical force resulted in greater deformation of the piezo catalyst as well as a higher level of free radical production.

### 3.3.4. Effect of ultrasonic time on the piezo degradation efficiency

Fig. 5 d illustrates how ultrasonic time influences asphaltene degradation. The ultrasonic time can have a significant impact on the degradation efficiency of asphaltene by piezo catalysts. Degradation efficiency can generally be enhanced by prolonged ultrasonic exposure

times. According to the results, 71.6 % of asphaltene was degraded during 15 min of ultrasonic vibration. ADE% was increased to 79.4% by extending the ultrasonic time to 30 min. Following a 60 min and 120 min piezo degradation test, the ADE% reached 90.2 % and 92.4 %, respectively. After 60 min, the ADE% was almost constant. Increased ultrasonic time resulted in higher degradation rates because more cavitation bubbles are formed when ultrasonic waves are applied for a longer duration, resulting in more reactive species. It should be noted, however, that there is a threshold beyond which further increases in ultrasonic time may not significantly enhance degradation efficiency. The reason for this is that, after a certain point, the concentration of reactive species reaches a saturation point, which limits the amount of further degradation that can occur.

### 3.4. Stability and reusability of $\text{Ni}_x\text{Mn}_y\text{O}$ piezo catalysts

In environmental remediation and industrial processes, catalyst reusability is of great importance. The reusability of catalysts is highly valued for a number of reasons, including cost-effectiveness, process efficiency, sustainability, scalability, and waste reduction. The cost of producing or acquiring catalysts may be high, particularly if they contain rare or precious metals. It is possible to extend the lifespan of catalysts by reusing them, thereby reducing the need for frequent replacement or replenishment which leads to cost savings. Catalysts that are reusable contribute to sustainable practices by reducing resource consumption and waste production. The use of catalysts repeatedly reduces the demand for raw materials and energy-intensive production processes. Catalytic performance is maintained over time, allowing continuous operation and improved productivity. Consequently, production costs, reaction times, and energy requirements can be minimized. Using reusable catalysts reduces the amount of waste generated by reducing the amount of catalyst material that needs to be discarded after each use. As a result, this is especially beneficial when dealing with hazardous or environmentally harmful catalysts, since it reduces the risk associated with their disposal.

Based on the results shown in Fig. 6, N3 exhibits a high degree of reusability. N3 degraded 92.4 percent of asphaltene in the first run. As a

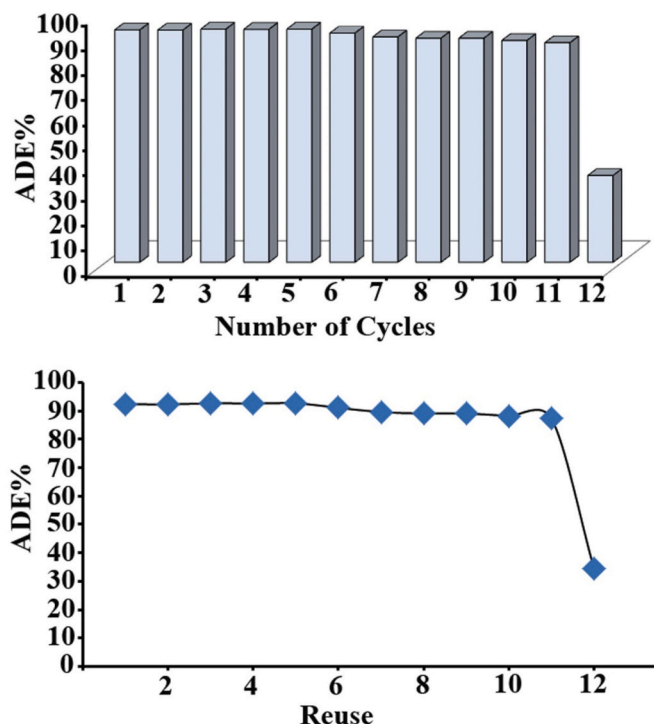


Fig. 6. Reusability of  $\text{Ni}_x\text{Mn}_y\text{O}$  as piezo catalyst in degradation of asphaltene.

result of reusing it in the degradation of asphaltene, the ADE% slightly decreased to 92.3%. Therefore, the ADE% remains constant and this difference may be due to human error. As a result of reusing N3 in the third run, an ADE% of 92.7% was achieved. As a result of the fourth run, an ADE% of 92.6% was achieved. The results indicate that ADE% was almost constant for the first six runs, but slightly decreased for the first eleven runs. In the 12th cycle of reusing N3, the ADE% had dropped to 34.5%.

### 3.5. Kinetic and thermodynamic of asphaltene degradation by piezo catalyst

The degradation of asphaltene using piezoelectric materials involves both kinetic and thermodynamic factors. Surface area and the number of reactive species are two factors that may influence the kinetics of piezo asphaltene degradation. The degradation of asphaltene follows the second-order model after fitting the reaction rate with zero, first, and second-order models. According to the results shown in Fig. 7a, b and Table 3, the  $R^2$  for the second-order kinetic model was closer to 1 at all three temperatures (293 K, 303 K, and 313 K). This indicated that the asphaltene degradation pathway significantly depends on asphaltene

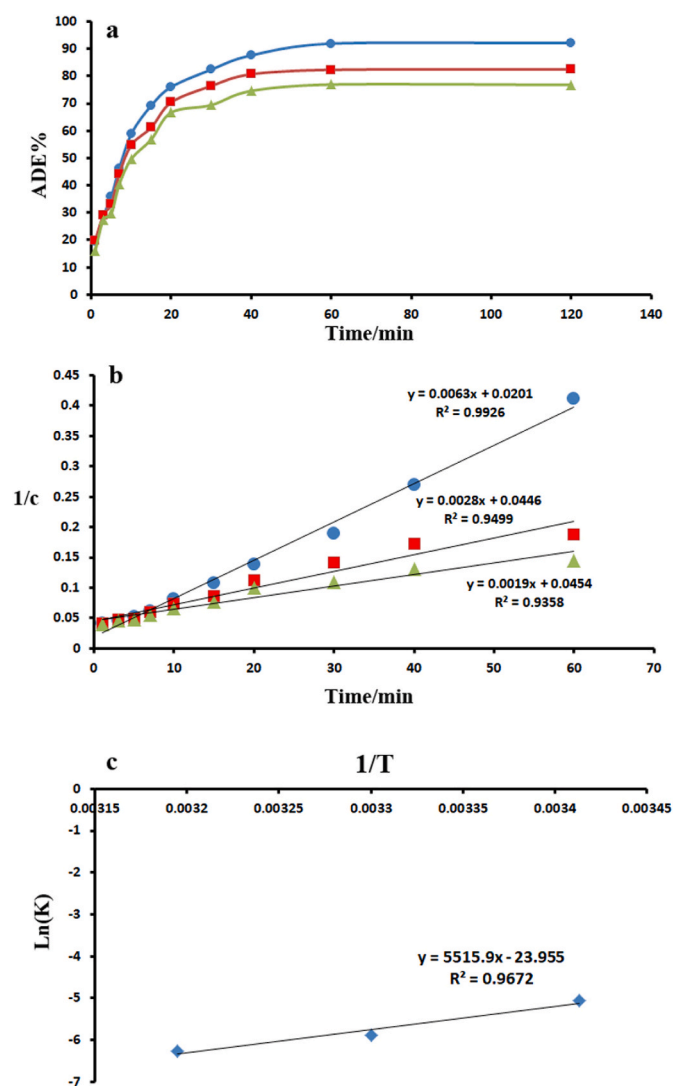


Fig. 7. a) ADE% over time at 293 K, 303 K, and 313 K, b) Second order fitting for asphaltene degradation at 293 K, 303 K, and 313 K, c) LNK Vs  $1/T$  Plot for the experimental data for the evaluation of thermodynamic Parameters of the degradation of asphaltene.

Table 3

R2 for zero, first, and second order kinetic of degradation of asphaltene by  $Ni_xMn_yO$  piezo catalysts.

Reaction temperature, °C	$R^2$ zero order	$R^2$ First order	$R^2$ second order	$K_2$ ( $M^{-1} \cdot min^{-1}$ )
20	0.76	0.94	0.99	0.0063
30	0.75	0.87	0.95	0.0028
40	0.75	0.86	0.94	0.0019

concentration. It was found that by increasing the temperature of the reaction, the rate constant (K) decreased. K was  $0.0063 M^{-1} \cdot min^{-1}$  when the piezo degradation reaction was conducted at 293 K. This value was decreased to  $0.0028 M^{-1} \cdot min^{-1}$  when the piezo degradation reaction was conducted at 303 K, and to  $0.0019 M^{-1} \cdot min^{-1}$  when it was conducted at 313 K.

Eqs (1)–(3) were used to study the thermodynamics of piezo degradation of asphaltene, including the changes in enthalpy ( $\Delta H^\circ$ ), entropy ( $\Delta S^\circ$ ), and Gibbs free energy ( $\Delta G^\circ$ ).

$$Kc = \frac{qe}{ce} \quad (1)$$

$$\ln(Kc) = -\frac{\Delta H^\circ}{R} \left(\frac{1}{T}\right) + \left(\frac{\Delta S^\circ}{R}\right) \quad (2)$$

$$\Delta G = -RTL \ln K \quad (3)$$

A thermodynamic study for asphaltene degradation by  $Ni_xMn_yO$  piezo catalysts indicated that the reaction is exothermic.  $\Delta H$  value for piezo degradation of asphaltene was  $-45.85 kJ \cdot mol^{-1}$ . Here, R ( $8.314 J \cdot mol^{-1} \cdot K^{-1}$ ) is the universal gas constant, T (K) is the temperature, and Kc is the equilibrium constant according to Eq. (2). With the slope and intercept of the van Hoff diagram calculated using the  $\ln Kc$  as a function of  $1/T$ , we can find the  $\Delta H^\circ$  and  $\Delta S^\circ$  values using the slope and intercept from the diagram (Fig. 7 c). By using Eq. (3), it is possible to calculate  $\Delta G^\circ$  at the desired temperature. In Supplementary Table S1, the results of the calculation of thermodynamic variables at different temperatures are presented. In standard conditions, a positive  $\Delta G^\circ$  indicates that a chemical reaction is not spontaneous. In a chemical reaction under standard conditions, a negative  $\Delta S^\circ$  (Delta S standard) indicates a decrease in entropy during piezo degradation of asphaltene.

### 3.6. Mechanism of asphaltene degradation by piezo catalyst

In order to design effective pollution remediation, process optimization, and predict degradation pathways, it is essential to understand the reaction mechanism of asphaltene degradation. For this purpose, we performed a free radical scavenger experiment using benzoquinone (BQ) to scavenge superoxide radicals,  $Na_2$ -EDTA to catch holes, and isopropanol (IPA) to capture hydroxyl radicals [55,56]. Additionally, we used N3 as a piezo catalyst in a solution containing 30 ppm asphaltene. Based on the results presented in Fig. 8 a, when BQ was used in asphaltene degradation, ADE% decreased from 92.4% to 75%. As a result of adding  $Na_2$ -EDTA to the piezo-catalyst system, the ADE% decreased to 37%. In addition, when IPA was added to the system, an ADE% of 35% was obtained. Results show that superoxide radicals, holes, and hydroxyl radicals are involved in the degradation of asphaltene by  $Ni_xMn_yO$  piezo catalysts. However, hydroxyl radicals and holes are responsible for the majority of asphaltene degradation. In light of these results, we have proposed a mechanism for the piezo-degradation of asphaltene in toluene using  $Ni_xMn_yO$  piezo catalysts (Fig. 8 b). In accordance with the catalyst mechanism, electrons, and holes are generated as a result of ultrasonic vibration stimulating  $Ni_xMn_yO$  piezo catalyst. A portion of the holes are capable of reacting directly with asphaltene and degrading it. Furthermore, the hole produced hydroxyl radicals, which could attach to asphaltene and cause degradation. There are two possible sources for OH to produce OH radicals. It's worth

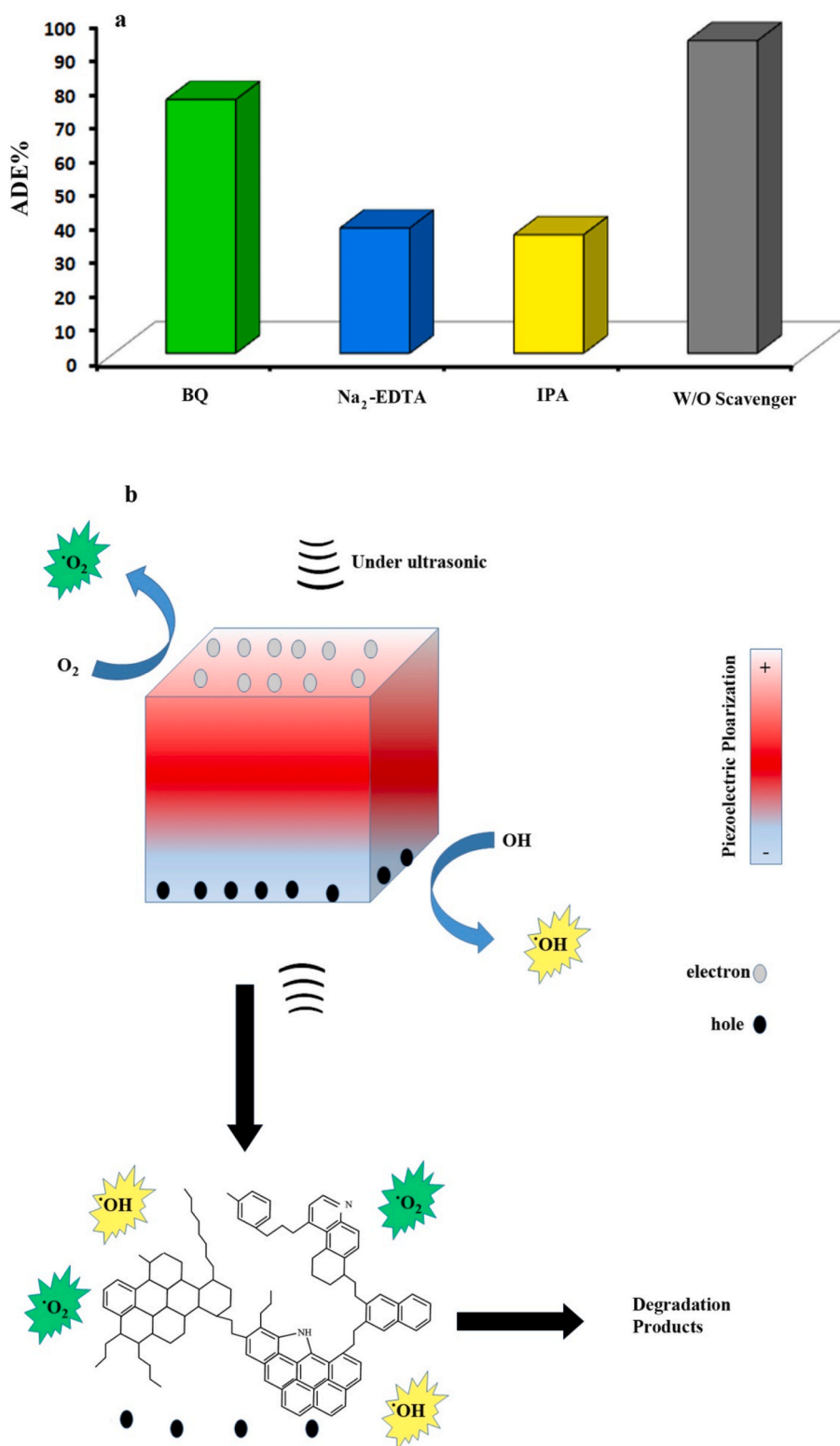


Fig. 8. a) The degradation of asphaltene by Ni<sub>x</sub>Mn<sub>y</sub>O was investigated in the presence of BQ, EDTA, and IPA as scavengers. b) The proposed mechanism for the degradation of asphaltene by Ni<sub>x</sub>Mn<sub>y</sub>O under the influence of ultrasonic radiation.

noting that asphaltenes contain an OH functional group that has the potential to react with holes and generate OH radicals. In addition, they can act as a surfactant with a nonpolar part that is attracted to oil and a polar part that can bind with water or polar compounds. Consequently, they may capture some water molecules, which could then react with holes and produce OH radicals. In addition, an electron may react with

oxygen to produce superoxide free radicals, which could contribute to the degradation of asphaltene.

#### 4. Conclusion

In this study we developed a new method for degradation of

asphaltene that is fast, clean, and cost-effective. Here Ni<sub>x</sub>Mn<sub>y</sub>O piezo catalyst was used to degradation of asphaltene under ultrasonic irradiation. PFM results showed that the Ni<sub>x</sub>Mn<sub>y</sub>O piezo catalyst has d33 of about 350 pC/N indicated a high piezo response in the champion catalyst. Results showed that up to 94.7 % of asphaltene could be degraded by adjusting conditions in the present of a piezo catalyst, while bare ultrasonic treatment only degrades around 1% of asphaltene. Results showed that synthesis parameter including off time in each microwave cycling, precursor concentration, ammonia concentration, microwave power and time have significant effect on ADE%. Results showed that asphaltene degradation was increased by increasing off time, precursor concentration, and microwave power. Furthermore, operation parameters including dosage of Ni<sub>x</sub>Mn<sub>y</sub>O piezo catalyst, asphaltene concentration, ultrasonic power and time influence the asphaltene degradation yield. Based on the results, ADE% was increased by increasing dosage of Ni<sub>x</sub>Mn<sub>y</sub>O piezo catalyst, increasing ultrasonic power and time, and decreasing asphaltene concentration.

The results of the kinetic studies indicated that Ni<sub>x</sub>Mn<sub>y</sub>O is able to degrade asphaltene following second-order laws. Furthermore, the study demonstrated that the degradation pathway is significantly affected by asphaltene concentration. It was found that by increasing the temperature of the reaction, the rate constant (K) decreased. K was 0.0063 M<sup>-1</sup> min<sup>-1</sup> when the piezo degradation reaction was conducted at 293 K. A thermodynamic study for asphaltene degradation by Ni<sub>x</sub>Mn<sub>y</sub>O piezo catalysts indicated that the reaction is exothermic. ΔH value for piezo degradation of asphaltene was -45.85 kJ mol<sup>-1</sup>.

Based on the scavenger experimental results, when BQ was used in asphaltene degradation, ADE% decreased from 92.4% to 75%. As a result of adding Na<sub>2</sub>-EDTA to the piezo-catalyst system, the ADE% decreased to 37%. In addition, when IPA was added to the system, an ADE% of 35% was obtained. Results show that superoxide radicals, holes, and hydroxyl radicals are involved in the degradation of asphaltene by Ni<sub>x</sub>Mn<sub>y</sub>O piezo catalysts. However, hydroxyl radicals and holes are responsible for the majority of asphaltene degradation.

#### CRedit authorship contribution statement

**Wrea Muhammed Ibrahim:** Methodology, Data curation. **Omid Amiri:** Writing – original draft, Supervision, Conceptualization. **Sangar S. Ahmed:** Writing – review & editing, Methodology, Conceptualization. **Hunar Yasin Muhammed:** Methodology, Data curation. **Peshawa H. Mahmood:** Methodology. **Karzan A. Qurbani:** Writing – review & editing. **Nabaz A. Abdulrahman:** Methodology. **Karim A. Younis:** Methodology. **Peshang Kh Omer:** Methodology.

#### Declaration of competing interest

The authors declare that they have no known competing financial interests or personal relationships that could have appeared to influence the work reported in this paper.

#### Data availability

Data will be made available on request.

#### Acknowledgements

Authors are grateful to the council of University of Cihan-Erbil to support this work.

#### Appendix A. Supplementary data

Supplementary data to this article can be found online at <https://doi.org/10.1016/j.rineng.2024.101938>.

#### References

- [1] H. Doryani, M.R. Malayeri, M. Riazi, Visualization of asphaltene precipitation and deposition in a uniformly patterned glass micromodel, *Fuel* 182 (2016) 613–622.
- [2] M. Tavakkoli, M.R. Grimes, X. Liu, C.K. Garcia, S.C. Correa, Q.J. Cox, F.M. Vargas, Indirect method: a novel technique for experimental determination of asphaltene precipitation, *Energy Fuels* 29 (5) (2015) 2890–2900.
- [3] F.M. Vargas, J.L. Creek, W.G. Chapman, On the development of an asphaltene deposition simulator, *Energy Fuels* 24 (4) (2010) 2294–2299.
- [4] Kh Gharbi, Kh Benyounes, M. Khodja, Removal and prevention of asphaltene deposition during oil production: a literature review, *J. Petrol. Sci. Eng.* 158 (2017) 351–360.
- [5] A. Khormali, R. Moghadasi, Y. Kazemzadeh, I. Struchkov, Development of a new chemical solvent package for increasing the asphaltene removal performance under static and dynamic conditions, *J. Petrol. Sci. Eng.* 206 (2021) 109066.
- [6] A. Khormali, A.R. Sharifov, D.I. Torba, The control of asphaltene precipitation in oil wells, *Petrol. Sci. Technol.* 36 (2018) 443–449.
- [7] M. Salehzadeh, A. Akherati, F. Ameli, B. Dabir, Experimental study of ultrasonic radiation on growth kinetic of asphaltene aggregation and deposition, *Can. J. Chem. Eng.* 94 (2016) 2202–2209.
- [8] S.M. Campen, S.J. Moorhouse, J.S.S. Wong, Effect of aging on the removal of asphaltene deposits with aromatic solvent, *Langmuir* 35 (37) (2019) 11995–12008.
- [9] Y. Chi, J. Yang, C. Sarica, N. Daraboina, A critical review of controlling paraffin deposition in production lines using chemicals, *Energy Fuels* 33 (4) (2019) 2797–2809.
- [10] E. Otumudia, H. Hamidi, P. Jadhawar, K. Wu, Effects of reservoir rock pore geometries and ultrasonic parameters on the removal of asphaltene deposition under ultrasonic waves, *Ultrason. Sonochem.* 83 (2022) 105949.
- [11] A. Khormali, Asphaltene precipitation and inhibition in carbonate reservoirs, *Petrol. Sci. Technol.* 35 (2017) 515–521.
- [12] A. Khormali, Effect of Water Cut on the Performance of an Asphaltene Inhibitor Package: Experimental and Modeling Analysis, *Petroleum Science and Technology* 40, 2022, pp. 2890–2906.
- [13] S.I. Ali, Z. Awan, Sh M. Lalji, Laboratory evaluation experimental techniques of asphaltene precipitation and deposition controlling chemical additives, *Fuel* 310 (Part A) (2022) 122194.
- [14] K. Guo, H. Li, Zh Yu, In-situ heavy and extra-heavy oil recovery: a review, *Fuel* 185 (2016) 886–902.
- [15] S.I. Ali, Sh M. Lalji, J. Haneef, Us Ahsan, S.M. Tariq, S.T. Tirmizi, R. Shamim, Critical analysis of different techniques used to screen asphaltene stability in crude oils, *Fuel* 299 (2021) 120874.
- [16] L.C.R. Junior, M.S. Ferreira, A.C. da S. Ramos, Inhibition of asphaltene precipitation in Brazilian crude oils using new oil soluble amphiphiles, *J. Petrol. Sci. Eng.* 51 (2006) 26–36.
- [17] R. Hashemi, N.N. Nassar, P.P. Almao, Nanoparticle technology for heavy oil in-situ upgrading and recovery enhancement: opportunities and challenges, *Appl. Energy* 133 (2014) 374–387.
- [18] T.G. Ambaye, A. Chebbi, F. Formicola, Sh Prasad, F.H. Gomez, A. Franzetti, M. Vaccari, Remediation of soil polluted with petroleum hydrocarbons and its reuse for agriculture: recent progress, challenges, and perspectives, *Chemosphere* 293 (2022) 133572.
- [19] J. Tang, X. Lu, Q. Sun, W. Zhu, Aging effect of petroleum hydrocarbons in soil under different attenuation conditions, *Agric. Ecosyst. Environ.* 149 (2012) 109–117.
- [20] S.S.K. Singh, A.K. Haritash, Polycyclic aromatic hydrocarbons: soil pollution and remediation, *Int. J. Environ. Sci. Technol.* 16 (2019) 6489–6512.
- [21] I. Ch Ossai, A. Ahmed, A. Hassan, F. Sh Hamid, Remediation of soil and water contaminated with petroleum hydrocarbon: a review, *Environ. Technol. Innovat.* 17 (2020) 100526.
- [22] S.P. Maletić, J.M. Beljin, S.D. Rončević, M.G. Grgić, B.D. Dalmacija, State of the art and future challenges for polycyclic aromatic hydrocarbons in sediments: sources, fate, bioavailability and remediation techniques, *J. Hazard Mater.* 365 (2019) 467–482.
- [23] J.D. Aparicio, E.E. Raimondo, J.M. Saez, S.B. Costa-Gutierrez, A. Álvarez, C. S. Benimeli, M.A. Polti, The current approach to soil remediation: a review of physicochemical and biological technologies, and the potential of their strategic combination, *J. Environ. Chem. Eng.* 10 (2) (2022) 107141.
- [24] Ch Lin Yap, S. Gan, H. Kiat Ng, Evaluation of solubility of polycyclic aromatic hydrocarbons in ethyl lactate/water versus ethanol/water mixtures for contaminated soil remediation applications, *J. Environ. Sci.* 24 (6) (2012) 1064–1075.
- [25] X. Zhao, Y. Gong, S.E. O'Reilly, D. Zhao, Effects of oil dispersant on solubilization, sorption and desorption of polycyclic aromatic hydrocarbons in sediment-seawater systems, *Mar. Pollut. Bull.* 92 (2015) 160–169.
- [26] I.B. Ivshina, M.S. Kuyukina, A.V. Krivoruchko, A.A. Elkin, S.O. Makarov, C. J. Cunningham, T.A. Peshkur, R.M. Atlasd, J.C. Philp, Oil spill problems and sustainable response strategies through new technologies, *Environ. Sci.: Process. Impacts* 17 (2015) 1201–1219.
- [27] S.M. Bamforth, I. Singleton, Bioremediation of polycyclic aromatic hydrocarbons: current knowledge and future directions, *J. Chem. Technol. Biotechnol.* 80 (2005) 723–736.
- [28] Sh Tu, Y. Guo, Y. Zhang, Ch Hu, T. Zhang, T. Ma, H. Huang, Piezocatalysis and Piezo-Photocatalysis: Catalysts Classification and Modification Strategy, Reaction Mechanism, and Practical Application, *Advanced Functional Materials* 30, Special Issue: Advanced Functional Materials for Organoids and Tissues, 2020 2005158.

- [29] O. Amiri, Kh Salar, P. Othman, T. Rasul, D. Faiq, M. Saadat, Purification of wastewater by the piezo-catalyst effect of PbTiO<sub>3</sub> nanostructures under ultrasonic vibration, *J. Hazard Mater.* 394 (2020) 122514.
- [30] O. Amiri, G.L. Abdulla, Ch M. Burhan, H.H. Hussein, A.M. Azhdarpoor, M. Saadat, M. Joshaghani, P.H. Mahmood, Boost piezocatalytic activity of BaSO<sub>4</sub> by coupling it with BaTiO<sub>3</sub>, Cu:BaTiO<sub>3</sub>, Fe:BaTiO<sub>3</sub>, S:BaTiO<sub>3</sub> and modify them by sucrose for water purification, *Sci. Rep.* 12 (2022) 20792.
- [31] S.S. Ahmed, O. Amiri, K.M. Rahman, S.J. Ismael, N.S. Rasul, D. Mohammad, K. A. Babakr, N.A. Abdulrahman, Studying the mechanism and kinetics of fuel desulfurization using CexOy/NiOx piezo-catalysts as a new low-temperature method, *Sci. Rep.* 13 (2023) 7574.
- [32] J. Zhang, Ch Wang, Ch Bowen, Piezoelectric effects and electromechanical theories at the nanoscale, *Nanoscale* 6 (2014) 13314–13327.
- [33] M. Dai, Zh Wang, F. Wang, Y. Qiu, J. Zhang, Ch-Y. Xu, T. Zhai, W. Cao, Y. Fu, D. Jia, Y. Zhou, P.-A. Hu, Two-dimensional van der Waals materials with aligned in-plane polarization and large piezoelectric effect for self-powered piezoelectric sensors, *Nano Lett.* 19 (2019) 5410–5416.
- [34] X.Z. Jiang, Y.C. Li, J. Wang, J.C. Li, Electromechanical modeling and experimental analysis of a compression-based piezoelectric vibration energy harvester, *Int. J. Soc. Netw. Min.* 5 (2014) 152–168.
- [35] K.A. Babakr, O. Amiri, L.J. Guo, M.A. Rashi, P.H. Mahmood, Kinetic and thermodynamic study in piezo degradation of methylene blue by SbSI/Sb<sub>2</sub>S<sub>3</sub> nanocomposites stimulated by zirconium oxide balls, *Sci. Rep.* 12 (2022) 15242.
- [36] O. Amiri, A. Abdalrahman, G. Jangi, H.A. Ahmed, S.H. Hussein, M. Joshaghani, R. Z. Mawlood, M. Salavati-Niasari, Convert mechanical energy to chemical energy to effectively remove organic pollutants by using PTO catalyst, *Separ. Purif. Technol.* 283 (2022) 120235.
- [37] K. Kubota, Y. Pang, A. Miura, A.H. Ito, Redox reactions of small organic molecules using ball milling and piezoelectric materials, *Science* 366 (2019) 1500–1504.
- [38] M.A.A.H. Allah, H.A. Alshamsi, Facile green synthesis of ZnO/AC nanocomposites using *Pontederia crassipes* leaf extract and their photocatalytic properties based on visible light activation, *J. Mater. Sci. Mater. Electron.* 34 (2023) 1263.
- [39] A.A. kadhem, H.A. Alshamsi, Biosynthesis of Ag-ZnO/rGO nanocomposites mediated *Ceratophyllum demersum* L. leaf extract for photocatalytic degradation of Rhodamine B under visible light, *Biomass Convers. Biorefin.* 12 (2023) 346–352.
- [40] H.A. Khayoon, M. Ismael, A. Al-nayili, H.A. Alshamsi, Fabrication of LaFeO<sub>3</sub>-nitrogen deficient g-C<sub>3</sub>N<sub>4</sub> composite for enhanced the photocatalytic degradation of RhB under sunlight irradiation, *Inorg. Chem. Commun.* 157 (2023) 111356.
- [41] J. Liu, W. Qi, M. Xu, T. Thomas, S. Liu, M. Yang, Piezocatalytic techniques in environmental remediation, *Angew. Chem.* 62 (2023) e202213927.
- [42] Ch Wang, F. Chen, Ch Hu, T. Ma, Y. Zhang, H. Huang, Efficient piezocatalytic H<sub>2</sub>O<sub>2</sub> production of atomic-level thickness Bi<sub>4</sub>Ti<sub>3</sub>O<sub>12</sub> nanosheets with surface oxygen vacancy, *Chem. Eng. J.* 431 (2022) 133930.
- [43] X. Ning, A. Hao, Y. Cao, J. Hu, J. Xie, D. Jia, Effective promoting piezocatalytic property of zinc oxide for degradation of organic pollutants and insight into piezocatalytic mechanism, *J. Colloid Interface Sci.* 577 (2020) 290–299.
- [44] L. Chen, X. Dai, Xiaojing Li, J. Wang, H. Chen, Xin Hu, H. Lin, Y. He, Y. Wu, M. Fan, A novel Bi<sub>2</sub>S<sub>3</sub>/K<sub>2</sub>Ta<sub>0.75</sub>Nb<sub>0.25</sub>O<sub>3</sub> nanocomposite with high efficiency for photocatalytic and piezocatalytic N<sub>2</sub> fixation, *J. Mater. Chem. A* 9 (2021) 13344–13354.
- [45] T. Cheng, W. Gao, H. Gao, Sh Wang, Z. Yi, X. Wang, H. Yang, Piezocatalytic degradation of methylene blue, tetrabromobisphenol A and tetracycline hydrochloride using Bi<sub>4</sub>Ti<sub>3</sub>O<sub>12</sub> with different morphologies, *Mater. Res. Bull.* 141 (2021) 111350.
- [46] G.A. Babu, G. Ravi, T. Mahalingam, M. Kumaresavanjic, Y. Hayakawad, Influence of microwave power on the preparation of NiO nanoflakes for enhanced magnetic and supercapacitor applications, *Dalton Trans.* 44 (2015) 4485–4497.
- [47] N.F.A. Neto, T.B.O. Nunes, M. Li, E. Longo, M.R.D. Bomio, F.V. Motta, Influence of microwave-assisted hydrothermal treatment time on the crystallinity, morphology and optical properties of ZnWO<sub>4</sub> nanoparticles: photocatalytic activity, *Ceram. Int.* 46 (2020) 1766–1774.
- [48] N. Bisht, S.S. Rao, S. Deshawal, P.K. Khanna, Novel microwave synthesis of copper chromite nanoparticles, *Inorg. Chem. Commun.* 134 (2021) 109072.
- [49] Y. Yao, H. Chen, Chao Lian, F. Wei, D. Zhang, G. Wu, B. Chen, Sh Wang, Fe, Co, Ni nanocrystals encapsulated in nitrogen-doped carbon nanotubes as Fenton-like catalysts for organic pollutant removal, *J. Hazard Mater.* 314 (2016) 129–139.
- [50] T. Novakov, S.G. Chang, A.B. Harker, Sulfates as pollution particulates: catalytic formation on carbon (Soot) particles, *Science* 186 (1974) 259–261.
- [51] D. Chen, Y. Cheng, N. Zhou, P. Chen, Y. Wang, K. Li, Sh Huo, P. Cheng, P. Peng, R. Zhang, L. Wang, H. Liu, Y. Liu, R. Ruan, Photocatalytic degradation of organic pollutants using TiO<sub>2</sub>-based photocatalysts: a review, *J. Clean. Prod.* 268 (2020) 121725.
- [52] H. Dong, G. Zeng, L. Tang, Ch Fan, Ch Zhang, X. He, Y. He, An overview on limitations of TiO<sub>2</sub>-based particles for photocatalytic degradation of organic pollutants and the corresponding countermeasures, *Water Res.* 79 (2015) 128–146.
- [53] J. Cai, X. Huai, R. Yan, Y. Cheng, Numerical simulation on enhancement of natural convection heat transfer by acoustic cavitation in a square enclosure, *Appl. Therm. Eng.* 29 (2009) 1973–1982.
- [54] A. Khoobi, M. Salavati-Niasari, O. Amiri, Ultrasonic synthesis and characterization of SnFe<sub>1.2</sub>O<sub>1.9</sub>/GO nanocomposite: application of multivariate optimization in magnetic solid-phase extraction, *J. Alloys Compd.* 858 (2021) 157745.
- [55] O. Amiri, S.S. Ahmed, K.A. Younis, K.M. Rahman, S.J. Ismael, N.S. Rasul, K. A. Babakr, N.A. Abdulrahman, Pizo- catalytic desulfurization of model and real fuel samples over NiO/MnxOy nano-composite at room temperature: mechanism and kinetic behind it, *Fuel* 344 (2023) 128065.
- [56] O. Amiri, F. Beshkar, S.S. Ahmed, A. Rafiei-Miandashti, P.H. Mahmood, A. A. Dezaye, Novel flower-like (Bi(Bi<sub>2</sub>S<sub>3</sub>)<sub>9</sub>I<sub>3</sub>)<sub>2/3</sub> nanostructure as efficient photocatalyst for photocatalytic desulfurization of benzothiophene under visible light irradiation, *Adv. Powder Technol.* 32 (4) (2021) 1088–1098.